Environ Monit Assess (2018) 190: 309
https://doi.org/10.1007/s10661-018-6688-1

Dynamics of land change: insights from a three-level intensity analysis of the Legedadie-Dire catchments, Ethiopia

Yilikal Anteneh · Till Stellmacher · Gete Zeleke · Wolde Mekuria · Ephrem Gebremariam

Received: 1 June 2017 / Accepted: 16 April 2018 / Published online: 25 April 2018
© Springer International Publishing AG, part of Springer Nature 2018

Abstract Earlier studies on land change (LC) have focused on size and magnitude, gains and losses, or land transfers between categories. Therefore, these studies have failed to simultaneously show the complete LC processes. This paper examines LCs in the Legedadie-Dire catchments in Oromia State, Ethiopia, using land-category maps with intensity analysis (IA) at three points in time. We comprehensively analyze LC to jointly encompass the rate, intensity, transition, and process. Thirty-meter US Geological Survey (USGS) Landsat imagery from 1986, 2000, and 2015 (< 10% cloud) is processed using TerrSet-LCM and ArcGIS. Six categories are identified using a maximum likelihood classification technique: settlement, cultivation, forest, water, grassland, and bare land. Then, classified maps are superimposed on the images to statistically examine changes with an IA. Considerable changes are observed among categories, except for water, between 1986–2000 and 2000–2015. Overall land change occurred quickly at first and then slowly in the second time interval. The total land area that exhibited change (1st ≈ 54% and 2nd ≈ 51%) exceeded the total area of persistence (1st ≈ 46% and 2nd ≈ 49%) across the landscape. Cultivation and human settlements were the most intensively increased categories, at the expense of grassland and bare ground. Hence, when grassland was lost, it tended to be displaced by cultivation more than other categories, which was also true with bare land. Annual intensity gains were active for forest but minimal for cultivation, implying that the gains of forest were associated with in situ reforestation practices and that the gains in cultivation were caused by its relatively large initial area under a uniform intensity concept. This study demonstrates that IA is valuable for investigating LC across time intervals and can help distinguish dormant vs. active and targeted vs. avoided land categories.

Keywords Land change · Classification · Intensity analysis · Interval · Transition · Dormant

Y. Anteneh (✉)
Geography and Environmental Studies, Arba Minch University (AMU), P.O. Box: 21, Arba Minch, Ethiopia
e-mail: yiliku100@live.com

T. Stellmacher
Center for Development Research (ZEF), University of Bonn, Bonn, Germany

G. Zeleke
Water and Land Resource Center (WLRC), P. O. Box: 3880, Addis Ababa, Ethiopia

W. Mekuria
International Water Management Institute (IWMI), P.O. Box 5689, Addis Ababa, Ethiopia

E. Gebremariam
Ethiopian Institute of Architecture, Building Construction, and City Development (EiABC), Addis Ababa University (AAU), P.O. Box: 518, Addis Ababa, Ethiopia

Introduction

Land cover and land use are closely linked. Land cover includes the attributes of the Earth's land surface and immediate subsurface, such as soil, topography, biota,

built-up areas, and water (Verburg et al. 2009). Thus, conversions constitute the replacement of one cover type by another and are measured by a transition from one land-cover category to another. Land use encompasses the purposes for which humans exploit land cover (Lambin and Geist 2008) and includes the manner in which the biophysical characteristics of the land are handled and the primary purpose behind that manipulation (Lambin and Geist 2008). Terrestrial land uses and land covers, and changes therein, are fundamental to many of the biophysical processes of environmental change at any spatial and temporal scale, qualifying "land change as a forcing function in global environmental change" (Turner 2006). Thus, these two concepts, i.e., land-use change and land-cover change, are referred to as "land change" hereafter in this manuscript.

Land change that is observed at any spatiotemporal scale involves complex synergy with changes that are seen at other analytical scales (Meyer and Turner 2002). Anthropogenic effects and natural processes trigger land changes that can have serious biophysical, ecological, socioeconomic, and political consequences (Wu et al. 2013). Therefore, recognizing the forms and manner of land change has become a central aim of studies that examine the complex interactions of coupled human-natural systems from a local to global scale (Aldwaik and Pontius 2013).

At any scale of land-change analysis, describing land-change patterns through the initial classification of land categories helps us more deeply understand the underlying changes. This approach facilitates the design of strategies for subsequent actions, including monitoring environmental changes, forecasting future trends, analyzing the consequences of land change, and managing natural resources (Turner II 2002). Therefore, the initial fundamental technique for characterizing perceived land change strongly influences the efficiency of land-change models and outputs (Aldwaik and Pontius 2013).

Many scientific land-change studies examined the magnitude of land conversion (Boyd & Danson 2005; Hansen et al. 2008a; Redo et al. 2011) and focused on one or a few aspects of land-change detection. Such detection can be the net change of a particular land category or its rate of change in a certain time interval, and these studies disregarded the processes and change transitions (Achard et al. 2002; Rogan & Chen 2004). This failure to identify transition processes, which are the main facilitator of land change, could be attributed to diverging interests and focuses of researchers. Some researchers concentrated on the net gains or losses of land change. Others were interested in the patterns of change from one land category to a succeeding category over a defined period, where the goal was to determine how much of the change was increasing, decreasing, or resisting change. Hence, various models' utility in assisting subsequent actions could be compromised.

An ideal unified approach for the detection and analysis of land change, as suggested by Macleod & Congalton (1998), follows some important steps. The first step is detecting whether the changes have prevailed; the second step is describing the nature of the change; the third step is quantifying the areal dimensions of the change; and the fourth step is assessing the spatial patterns and transition process of the change. Understanding and incorporating such versatile methods is necessary for enhanced resource management and improved decision-making (Aldwaik and Pontius 2013)

Accurately measuring underlying land-change characteristics and understanding change processes can help develop management strategies because observed changes can determine the hydrological and ecological processes that occur in catchments. Therefore, this research aims to characterize the land-change processes at three levels of analysis and generate more insightful information for practitioners and decision makers regarding the ongoing land-change processes in the Legedadie-Dire catchments. The Legedadie-Dire catchments are the primary source of the potable water supply (55%) to Addis Ababa (the capital of Ethiopia). In recent decades, Ethiopia in general, and in particular Addis Ababa near central Ethiopia, has experienced strong economic growth coupled with infrastructure development, population growth, and (sub-) urbanization processes (Dadi et al. 2015, 2016). This process is strongly mirrored in land-use changes in the case study area. Multiple development processes in both catchments have substantially altered the land-cover patterns and catchment parameters. Since the early 1990s, the Legedadie and Dire areas have undergone rapid socioeconomic development and have increasingly experienced urban influences given their proximity to Addis Ababa.

Detailed studies that can provide a full picture of land-change processes in these areas by integrating three levels of analysis have not yet been performed. Conducting such studies and generating science-based evidence can help planners and managers understand

the fundamental patterns of land transformation and evaluate the extent of stationarity of the changes over three decades, broken into three points in time, i.e., 1986, 2000, and 2015. Moreover, the findings of this study will be used as input for a parallel study that we are undertaking that aims to design a catchment-specific joint ecosystem-management plan.

Description of matrices

Matrices can be analyzed on maps of a specific area for the same set of land categories for at least two points in time (Gergel & Turner 2000; Munsi et al. 2010). These matrices support a broad range of studies on land change. The superimposed maps between any two points in time can generate a cross-tabulation matrix of rows and columns, where the rows represent land categories at the initial time and the columns represent land categories at the subsequent time. The records reveal the extent of land that transitioned from the first land category to the following category over a specified time interval (Pontius and Malizia 2004). Entries that are outside the diagonal line display land change and entries along the diagonal line exhibit land persistence (Takada et al. 2010; Romero-Ruiz et al. 2011).

The systematic examination of matrices can show the process in the patterns of detected land change in a manner that helps determine whether a pattern was initiated from more intensive or less intensive practices than from deceptively random or uniform actions. A straightforward, simple comparison among the records in the matrices does not indicate the course of observed patterns of change. Instead, signals of orderly exchanges between two intervals from matrices can be detected through systematically screening the size of land change from each category (Pontius and Malizia 2004). This technique helps further compare two land categories with different area proportions and their orderly transitions between categories.

Intensity analysis

Intensity analysis is a quantitatively summarized and cross-tabulated square transition matrix that is used to analyze maps of land categories from several points in time for a site. One matrix summarizes the changes in each time interval and includes the intensity of land-transition processes and possible explanations at three levels of detail: interval, category, and transition. This matrix helps compare the observed rates or intensity of changes with a uniform rate or the uniform intensity of changes that would exist if the annual rate or intensity of the changes were uniformly distributed across the entire temporal and spatial extent. Moreover, the need to consider all time steps together for a complete land-change analysis and assess various forms of land-change transitions makes intensity analysis a more powerful method (Aldwaik and Pontius 2012).

For instance, a transition from one land category "X" (grassland) to another land category "Y" (cropland) across two consecutive time intervals may exhibit different forms when compared at the first time interval (FTI) and the second time interval (STI). At least three possible outcomes could exist. First, the area of transition from "X" to "Y" in the FTI may exceed the extent of the transition in the STI. Second, the transition area in the FTI may be lower than the size of the transition in the STI. Third, the area of transition from "X" to "Y" across the two intervals could be equal to the uniform intensity and thus perfectly stationary. "Stationary" is defined as a resemblance in the land-change pattern between two or more time intervals. Of course, what is stationary at one level of measurement may not be stationary in another. Therefore, the major advantage of this method is its ability to consider all the above possible details in one comprehensive unified analysis. Correspondingly, the three levels of intensity analysis (Aldwaik and Pontius 2012) can describe and provide convincing reasons for these different forms of land transition.

Interval level intensity (ILI) analysis provides introductory information regarding whether land-change-transition processes occurred quickly or slowly or whether the overall annual rate of change could have increased/decreased across the entire landscape. Given the duration of time between the two time intervals and the uniformity of change among categories, three potential justifications may exist at this level of analysis (Aldwaik and Pontius 2012). First, the overall rate of change may accelerate in the FTI and thus a greater likelihood for a larger area transition from category "X" to category "Y" may exist in the FTI than in the STI. Second, the overall rate of change may accelerate in the STI; thus, a greater likelihood for a larger area transition from category "X" to category "Y" may exist in the STI than in the FTI. Third, the overall rate of change in both time intervals may appear uniform,

suggesting a more comparable transition from category "X" to category "Y" across the entire period.

Category level intensity (CLI) analysis can show additional features in the extent of the area transition between categories. This approach reveals whether the transition process between two land categories is active or dormant, and five potential justifications could exist at this level of analysis in addition to the three that were mentioned above. Fourth, category "Y" could have increased less actively across the entire landscape or become entirely dormant in the FTI. Fifth, category "X" could have decreased less actively across the entire landscape or become dormant in the FTI, perhaps because of a process that kept category "X" steady (such as strong conservation practices, as in the case of "X" = forest). Sixth, intensive gains in category "Y" could have been greater across the entire landscape in the FTI than in the STI. Seventh, intensive losses in category "X" could have been greater across the entire landscape in the FTI than in the STI. Eighth, the gains in category "Y" may be proportionate to the losses in category "X" during the FTI and STI. The fourth and fifth details of CLI explain why the extent of the area transition from category "X" to category "Y" during the FTI can fall behind that during the STI and reveals that the categories were dormant. The sixth and seventh category details justify the likelihood that the area transition from category "X" to category "Y" in the FTI exceeds the level in the STI and indicates that the categories were active.

Transition level intensity (TLI) analysis can further explain the extent of area-transition patterns in a manner that is more specific and technical and determines whether the transition process is targeting or avoiding a specific land category. Another five potential justifications exist at this level of analysis, following the preceding eight. Ninth, the gain in "Y" could have targeted "X" less intensively for takeover during the FTI compared to the available sizes of "X" for takeover by "Y." This effect can be triggered by a shift in the preferences and actions of "Y" that lead to the smaller change in "X" during the FTI than during the STI. However, "X" can still be targeted by other "non-Y" categories for takeover. Tenth, the loss of "X" avoids "Y" during the FTI more than during the STI, perhaps because of factors that are not convenient to "Y" entailed at "X" than to other categories during the FTI. Eleventh, the gain in "Y" could target "X" more intensively for takeover during the FTI than during the STI compared to the available sizes of "X" for takeover by "Y." Twelfth, the intensive loss in "X" targets "Y" during the FTI more than during the STI, perhaps because of factors that force "X" to recede for "Y" more than for other categories during the FTI. Thirteenth, the gain in "Y" during the FTI equally targets "X" during the STI. Thus, the extent of area transition from category "X" that is targeted by category "Y" during the FTI is comparable to that during the STI. Targeting a certain category for intensive loss is realized when the targeted category becomes suitable for the realization of the intended change in various forms and scales within physical to biological and spatial elements, such as slope, soil fertility, location, structure, adjacency, and materials.

The ninth and tenth explanations justify the TLI reasons for the small extent of the area transition from category "X" to category "Y" during the FTI compared to during the STI because of avoidance by the categories of interest. The eleventh and twelfth descriptions reveal the reason for the larger extent of the area transition from category "X" to category "Y" during the FTI than that during the STI because of targeting by the categories of interest.

Generally, intensity analysis between two or more points in time at the interval, category, and transition levels meets the requirements to capture the stationarity of any of the possible factors in an area transition. Accordingly, this study applies intensity analysis and assesses the rate, intensity, transition, and uniformity of land change between categories across two intervals.

Materials and methods

Study area

The catchments, Legedadie (207.3 km^2) and Dire (77.8 km^2), are located 30 km to the northeast of Addis Ababa within the Oromia National Regional State. Geographically, the Legedadie catchment is situated between 09° 01′ 50″ – 09° 12′ 56″ N latitude and 38° 56′ 35″ – 39° 04′ 13″ E longitude, whereas the Dire catchment lies between 09° 08′ 23″ – 09° 13′ 20″ N latitude and 38° 49′ 44″ – 38° 57′ 52″ E longitude. Both are upstream sub-catchments of the big Akaki River, which flows from northeast to southwest and constitutes the Awash River basin, one of the major inland drainage systems in Ethiopia.

According to the Legedadie-Legetafo city administration, the original settlement of the current Legedadie area was founded in 1935 during the Italian invasion and occupation as a garrison town. According to key informants, in 1935 when Italians invade Ethiopia, they settled on hilly land near the Laga-Dadhi River that was owned by a man called "Basha Ergete." After the liberation in 1941, more people settled into this area, and the Laga-Daadhii area expanded as a rural-urban settlement. Before the emergence of the town, these settlements were two separate areas under kebele farmers' associations. Laga Tafoo was a rural village, while Laga-Dadhi was a rural town in Berek District. In 1974, land was distributed to the peasant farmers and extra houses were transferred to the government by proclamation during the Derg regime.

These settlements combined to form the single town of Laga Tafo-Lege Dadhi in July 2006. The town also received legal recognition as a municipal town under Berek District in the northern Shewa Zone of the Oromia National Regional State. Historical sources show that this town received its present name from the two major rivers Legetafo and Legedadhi, which border and pass through the town and its surrounding areas.

Prior to early settlement, Laga-Daadhii (hereafter Legedadie) and its surrounding areas were once covered by dense forest and farmlands. The forest consisted of various indigenous trees, among which "*Tid*" (*Juniperus procera*), "Girar" (*Acacia senegal*), and "shola" (*Ficus sycomorus*) are the primary species. This forest was used as a home for various wild animals, including hyenas, antelope, foxes, and gazelles. Afterwards, increasing population and the intensification of farming activities in the area has led to severe deforestation.

Today, the landscape units that characterize the catchments include volcanic mountains, which range from 2402 to 3240 m above sea level. The major physiographic units are dissected mountains, hills, steep to undulating foot-slopes, gullies, valleys, and undulating to flat plains. The main land-cover units consist of settlements, moderately to intensively cultivated lands, grassland, eucalyptus-dominated and natural vegetation areas, bare soil, and water bodies. Most of the catchment landscapes are utilized for cropping and grazing for cattle.

Two seasonal patterns of weather that resemble those in Addis Ababa are exhibited. The weather is relatively cooler from June to December and warmer from February to May. The mean monthly temperature is between 16 °C in December (the coldest month) and 19 °C in May (the hottest month) throughout the year. The minimum and maximum registered temperatures at the Addis Ababa Bole station are 9 °C (in December) and 25 °C (from February through May), respectively (Andualem and Yonas 2008). The mean annual precipitation in the catchments is between 1000 and 1300 mm. In terms of the mean monthly precipitation, November is the driest (17.3 mm) and August is the wettest (222.3 mm). February is the windiest month, with a mean monthly wind speed of 15 km/h.

The catchments are characterized by high population-growth rates of nearly 7% per year. According to the 2011 master plan review (MPR) report,[1] the total population of the Legedadie and Dire catchments was 51,993. Disaggregated by catchment, the population was 38,314 in the Legedadie catchment and 13,679 in the Dire catchment, which were administratively divided into 24 and 9 rural kebeles, respectively (MPR 2011). Cultivation is the single most important livelihood (MPR 2011). However, the livelihoods of residents have become diversified with the recent rapid rates of urbanization, industrial growth, and flower growers in the area. The main cultivated crops are cereals (wheat, teff, and barley). Furthermore, different types of pulses (lentils, vetch, chickpeas, and fava beans) and vegetables (such as onions, garlic, and cabbage) are grown. The application of modern agricultural inputs among the farming communities in the catchments is rapidly expanding. The number of farm households that apply chemical fertilizer and pesticides in the Legedadie catchment in 2011 alone comprised 50.1 and 9.6%, respectively (MPR 2011). During the same period, catchment livestock populations in Tropical Livestock Units (1 TLU = 250 kg live-weight) were estimated at 39,000 TLU (MPR 2011).

The catchments are economically integrated with the nation's capital city of Addis Ababa. Given their location within a 30-km radius from the core of the metropolitan area of Addis Ababa, urban-rural interaction is more intense than in any other area of the country. The city has been supplied with natural resources such as fuelwood, water, and agricultural products (fresh vegetables, milk and dairy products, and cereals) alongside

[1] MPR (Master Plan Review). 2011. The Federal Democratic Republic of Ethiopia Catchment Rehabilitation and Awareness Creation for Geffersa, Legedadie, and Dire Catchment Areas, urban water supply and sanitation project report

parks and recreation services from the catchments. The flow of production, labor, and capital factors between Addis Ababa and the catchments is particularly important. Unskilled labor largely flows from rural areas to the city, and informal financial institutions (such as "idir" and "iqub") contribute the largest share of capital flows in both areas. The increased interaction with and access to the city economy in terms of capital, labor (public and private), goods, and services will subsequently trigger the transformation of portions of the catchment to peri-urban areas.

Image pre-processing and inherent challenges

Each land-cover type absorbs, reflects, or transmits electromagnetic energy, with the interactions differing between wavelengths. This pattern is termed as the Spectral Response Pattern (SRP). The basis for classification is thus to find some area of the electromagnetic spectrum where the interaction is uniquely different from other land cover that occurs in the image, which is referred to as the signature. The SRP is a characteristic of a particular land cover. According to Eastman (2016), however, consistently determining distinctive signatures in practice is difficult for the following reasons. (1) Changes in phonology during the growing period in most vegetation can lead to highly variable signatures because of a lack of a consistent SRP. (2) Changes in moisture and illumination as per the slope or the time of year can produce significantly different spectral response patterns. (3) Most land cover consists of mixtures of elementary features that are sensed as single pixels. For instance, a sensor can detect a combination of soil and plants in crops as a row-maize cultivation. Similarly, a mixture of deciduous and coniferous trees in a forest area can be detected in a single pixel. (4) The wavelengths in which a given sensor senses may not always be identical to those in which a land cover is most distinguishable. Today, several very important areas of the spectrum can be inspected via multispectral sensors, particularly for the distinction of vegetation. Nevertheless, many wavelengths could possibly discriminate many features; for instance, various rocks are not usually scrutinized, so huge functional areas have not yet been inspected.

Because of these problems, the remote sensing community has stressed the development of signatures with reference to specific examples within the image to be classified (Frantz et al. 2016) rather than relying on the use of more general libraries of characteristic spectral response patterns (Eastman 2016). These very specific examples are called training sites, which are so named because they are used to train the classifier on what to look for. By choosing examples from within the image itself (usually confirmed by a ground-truth visit, aerial photo and topographic maps), one can develop signatures that are specific to the available wavelengths (Eastman 2016). One can also avoid problems regarding variations in both the solar zenith angle and stage of the growing season (Tan et al. 2014). One can also select instances that are distinguishing features of the various cover class combinations that exist (Eastman 2016).

Despite this very pragmatic approach to the classification process, this problem remains a decision-based problem. We ask this process to create a definitive classification in the presence of considerable variations. For example, despite differences in the growth stage and soil background and the presence of intercropping, we ask the process to distill all variations in maize cropping into a single maize class (Eastman 2016).

Recently, however, concern has grown on relaxing this traditional approach in two areas, both of which are strongly represented in the TerrSet system that this study applies. The first is the development of soft classifiers, which are applied in this study, while the second improves the principles of multispectral sensing to hyperspectral sensing (Eastman 2016; Harsanyi et al. 1994). In the following section, only the former will be discussed.

Hard versus soft classifiers

Hard classifiers are also called traditional classifiers because they yield a hard decision regarding the identity of each pixel. Hard classifiers are so named because they all reach a hard (i.e., unambiguous) judgment regarding the category to which each pixel belongs. These classifiers are all based on a logic that describes the expected position of a class (based on training-site data) in what is known as band space and then gauges the location of each pixel to be classified in the same band space relative to these class positions.

In contrast, soft classifiers propose the extent to which a pixel belongs to each of the considered classes. Several factors support the use of soft classifiers. For instance, rather than deciding a pixel is either cultivation or grassland, its membership might be ranked within the land-cover categories, such as 0.57 in the cultivation

class and 0.43 in the grassland class, whereas a hard classifier might label the entire pixel as cultivation. One of the reasons for using a soft classifier is to determine the mixture of land-cover classes that are present. A pixel may contain 43% grassland cover and 57% cultivation if assume that these two classes are the only classes that are present; thus, this decision is a classification at the sub-pixel level.

Measuring and reporting the strength of evidence in support of the best conclusion is the second major reason for using soft classifiers. TerrSet presents distinctive soft classifiers that allow us to conclude, for example, that evidence for cultivation is present to a level of 0.26, that for grassland to 0.19 and some unidentified type to 0.55. This result immediately suggests that the evidence points to some other unidentified type despite the similarities between training sites for these two classes and the pixel.

A third reason for the use of soft classifiers is the use of models and GIS data layers to enhance the evidence that is used to reach a final judgment. For example, the probability that each pixel belongs to a residential land category can be extracted from the spectral data. Then, a GIS data layer of roads might be used to generate a map of distances from roads, and the probability of non-residential areas might be deduced (areas away from road networks are not likely to be residential). A stronger statement of the probability that this class exists can then be produced from these two lines of evidence. Subsequently, a final hard decision can be achieved by submitting the individual class-membership statements to an appropriate hardener, which is a decision procedure that selects the most likely alternative.

Selection and delineation of raining sites

Defining the areas that will be used as training sites for each land-cover class is the initial stage when performing a supervised classification. Appropriate care is taken when defining training sites for each land-cover class. Accordingly, a band with strong contrast (such as a near-infrared band) or a color composite is chosen. Once the strong contrast section is chosen, the image is displayed on the screen for out-scaling to produce good contrast and for on-screen digitizing to create vector files of training-site polygons. Only the areas within classes that are not mixed with other categories are chosen when defining a training site for a given land-cover class, and any pixels that are adjacent to other land categories are avoided by zooming in the area before digitizing. Moreover, at least 10 times as many pixels as bands in each classified image are digitized to accommodate enough pixels into a training site for each training class.

Spatial resolution and data and image classification

Spatial resolution

The information that one wishes to extract from imagery must be clear at the outset to choose an appropriate data set. The spatial resolution can be large or small depending on the purpose for which the remote sensing data can be processed and used (Carleer et al. 2005; Welch 1982). Each image data set has its advantages and disadvantages. On the one hand, studies have reported that processing and classifying low-resolution images poses a unique set of challenges (Yang 2013; Boyle et al. 2014). First, low-resolution images usually do not provide sufficient information because of their small number of pixels. Most of the texture details are discarded during data compression. Second, low-resolution images often have distortions and image artifacts, so performing dependable feature detection and extraction with pixelated textures and shapes becomes difficult (Yang 2013). Boyle et al. (2014) also noted that higher-resolution imagery can more accurately delineate cover classes, retain the patch shape, detect narrower linear patches, and identify smaller patches over low-resolution imagery. Such higher-resolution imagery products, however, are often costly and difficult to obtain, which reduces their use (Boyle et al. 2014).

On the other hand, the common belief that high-spatial-resolution images will always produce better interpretations may not always be true (Mahavir 2000). Although high-spatial-resolution images have been increasingly used to classify urban land cover based on traditional per-pixel spectral-based classification techniques, this approach often leads to poor classification performance (Lu et al. 2010). Specifically, the high spectral variations within the same land cover, the prevailing spectral confusion between various land covers, and the shadow problem of high-spatial-resolution images makes classification challenging (Mahavir 2000; Lu et al. 2010). This challenge primarily originates from two attributes. First, this type of classification is immensely more detailed than traditional classification systems because each pixel's spectral response is linked

with very specific earth and fabricated objects. Thus, no inherent generalization exists in low-resolution imagery. Second, the spectral confusion among different land covers and the high spectral variations within the same land cover can limit one's ability to discriminate between many Earth and manmade materials, even though the small pixel size dictates a high degree of classification specificity.

On the contrary, low-resolution images filter out unnecessary details when working at a metropolitan scale, so images with low spatial resolution are more useful than images with higher resolution, which makes classification more straightforward (Mahavir 2000). Thus, a careful balance must be sought between the classification purpose, image resolution, number of classes to be defined, and the ability to discriminate among the classes.

Data and image classification

Images from the Landsat Thematic Mapper (21 January 1986), Enhanced Thematic Mapper Plus (05 December 2000), and OLI TIRS (23 December 2015), all of which have 30-m spatial resolution were obtained from the US Geological Survey (USGS). Ideally, multi-temporal images for change monitoring should be from the same or consecutive seasons (Liu et al. 2015). However, large reflectance variations in vegetation exist because of phenology during the dry season in the tropics, which complicates land-cover change monitoring, although this approach is suitable to obtain cloud-free images (Liu et al. 2015). Compared to the dry season, the availability of haze- and cloud-free satellite images is restricted during the wet season. Dates during the middle of the dry season were selected to avoid clouds (< 10%) and reduce possible errors from seasonal differences between the time points.

Areal extent data (northeast of Addis Ababa) were extracted from Landsat scenes with Path 168 and Row 054. Image processing was conducted with the TerrSet geospatial monitoring and modeling system (Clark Labs, Worcester, MA, USA) and ENVI®Classic + IDL 64-bit image processing and analysis software from EXELIS Visual Information Solutions and ArcGIS 10.2 (Esri Eastern Africa Ltd., Kenya). Image composites were obtained using the near-infrared, red, and green bands of the imagery.

Landsat images had been previously georeferenced to the Universal Traverse Mercator (UTM) projection system, Zone 37 N with datum WGS 84, which was utilized throughout the analysis. A minor atmospheric correction was conducted by using the Quick Atmospheric Correction (QUAC), which is available with ENVI classic + IDL image processing. A radiometric correction was performed in all the Landsat images before classification. The Landsat imagery was spatially enhanced using a high-pass filter by traversing a three-by-three filter over the raster to enhance the passive edge features in the image. All the maps had the same spatial extent and the same categories. Each raster contained 310,861 pixels with 885 columns and 754 rows at the 30 m × 30 m resolution.

The land categories that were generated in this study had soft classifiers applied to them (at the sub-pixel level), followed by hard classifiers with a segmentation-classification procedure, a hybrid methodology between pixel-based and segment-based classification. This approach enabled us to reduce the challenge of differentiating ambiguous or similar classes on a single image (Eastman 2016). This procedure followed a supervised classification approach, with training-site information used to classify each image pixel. The initial soft classifier at the sub-pixel level helped determine the degree of membership to which each pixel belonged to each of the land-cover types. Thus, this procedure indicates the various proportions of land-cover representation to a single pixel instead of limiting the pixel to a single class. For example, this procedure can suggest that a pixel has a 0.69 probability of being cultivation, a 0.25 probability of being grassland, and a 0.06 probability of being bare land, which a hard classifier would normally label as cultivation. Unlike the traditional classification procedure, the outputs of a soft classifier are not a single classified land cover map, but rather they are a set of images (one image per class) that express for each pixel/sub pixel the degree of membership in the class in question, which would help differentiate ambiguous classes (Eastman 2016).

The land cover was initially classified through soft classifiers into 148 different clusters/colors of qualitative data relationships in the Terr Set Cluster module. The soft-classifier results were reevaluated to produce hard classifications for each pixel/sub pixel class by using the segmentation procedure. These classifiers were distinctive hard classifiers in the TerrSet geospatial monitoring and modeling system. Segmentation is a process that groups pixels/sub pixels that share a homogeneous spectral similarity.

Three sequential modules were applied for classification with this procedure. (1) The SEGMENTATION module created an image of segments from the set of images (outputs of the soft classifiers). Hence, the SEGMENTATION module grouped adjacent pixels and sub pixels into image segments according to their spectral similarity. Specifically, SEGMENTATION employed a watershed delineation approach to partition input imagery based on their variance. Based on variance similarity, a derived variance image was treated as a surface image that allocated pixels/sub pixels to specific segments. A moving window evaluated this similarity and segments were demarcated based on a stated similarity threshold. One standard deviation was applied as a threshold value in this research. Generally, the smaller the threshold, the more homogeneous the segments became, and the larger the threshold, the more heterogeneous and comprehensive the segments became. (2) The SEGTRAIN module interactively created training sites and signatures based on segments from SEGMENTATION. (3) The SEGCLASS module was derived from maximum likelihood classification, acting as a majority rule classifier based on the majority class within each segment. The clusters were subsequently classified into 6 dominant categories.

Information from aerial photographs of the Legedadie and Sendafa areas (1965, 1:50,000; 1969, 1:11,000; 1984, 1:50,000; and 1994, 1:8000), and a 1:50,000 topographic map of the area were obtained from the Ethiopian Mapping Agency to assist in the classification. Images from Google Earth and a reconnaissance survey that was conducted from December 2014 to April 2015 were used for the overall classification process. Recollections of elderly residents and the general landscape of the land cover during their lifetime in the catchment were collected during the reconnaissance survey, which all facilitated the classification procedure.

Moreover, the seasonal nature of agriculture in Ethiopia and the absence of land fallowing in the study catchments partially facilitated the classification efforts. The main agricultural regions in Ethiopia experience two rainy seasons, the Meher and the Belg, thus producing two crop seasons (Alemayehu et al. 2011). Meher is the main crop season, which extends from June to August and encompasses crops to be harvested in September. The Belg is the short rainy season, which extends from the last week of January to May (Eggenberger and Hunde 2001) and encompasses crops to be harvested in March (Alemayehu et al. 2011). Thus, farmers plow their lands in early December for Belg production. This approach also provides farmers the advantage of easy tillage right before the soil completely loses its moisture and becomes dry and hard.

In the central, southern and eastern areas of Ethiopia, less than 10% of the total grain production is produced from Belg crops (Eggenberger and Hunde 2001). Nevertheless, Belg rains are crucially important for the growth of Belg crops, seedbed preparation for short- and long-cycle Meher crops (main production season that extends from June to August), and planting of long-cycle cereal crops (maize, sorghum, millet). Usually, farmers plow twice before planting their Belg crops (Eggenberger and Hunde 2001). Thus, plowing usually begins in early December. The 16-day revisiting time of Landsat provides an opportunity to capture freshly plowed cultivation areas. SEGTRAIN can therefore partially generate images from these areas, which become the bases to develop training sites and signatures for the identification and classification of cultivated lands and then enable us to differentiate these areas from grasslands.

Fallowing is not practiced in the catchment because of the scarcity of land. Thus, we can avoid any challenges in terms of distinguishing fallow-cultivated land from grassland. Moreover, hard upstream exposed rocks characterize the bare lands in this area because of serious erosion. Plantations of eucalyptus forest were implemented in certain areas next to bare land to reduce soil erosion and inhibit the further expansion of bare land. These trees' purpose was for conservation, so these plantation forests are well protected from random access and harvesting, preventing any freshly slashed plantations. This phenomenon eliminates the presence of ambiguous classes and facilitates the detection of bare lands from surrounding eucalyptus plantations or grassland.

Methodological approach

This study incorporated different approaches to determine the important aspects of land change in its entirety. The locations where changes occurred and the magnitude of these changes were evaluated through maximum likelihood classification (object-based change detection methods). This method combines both spectral and textural data to extract and assign objects to a specific class to detect changes by comparing the independently

classified objects to multi-temporal images (Durieux et al. 2008). Additionally, the land change characteristics, areal extent, spatial patterns, and transition processes were investigated using an intensity analysis of pixel-by-pixel comparisons between two classified images to generate a full change matrix. Accordingly, land transitions between categories and across time intervals, patterns in the magnitude of land changes, and specific land-change transition processes were assessed.

A comprehensive methodological framework that moved from an interval to a categorical and then a transition level was used for the intensity analysis (Fig. 1). The overall land change across the entire period (three points in time from 1986 to 2015) was divided into two intervals (from 1986 to 2000 and from 2000 to 2015). Thus, the first level of analysis (interval level) focused on land change during this stage. As the name indicates, this level of analysis examined the size and annual rate of change across two time intervals.

The summation signs in the above boxes (Fig. 1) indicate the summation of both gross gains and gross losses (Table 1) when measuring slow vs. fast changes. The observed annual change intensity was compared to the uniform intensity that would exist if the annual changes were uniformly distributed across the entire time interval. The size and intensity of the gross gains and losses across categories were subsequently measured at the category level. The calculated intensities of the gross gains and losses and the observed intensities in each category were compared to a uniform intensity of annual change that would exist if the changes within each category across intervals were uniformly distributed over the entire landscape.

Finally, the size and intensity of the transitions among categories available for each transition were measured at the transition level. Categories, which were intensively avoided versus targeted for transition, could be identified by comparing each transition's observed

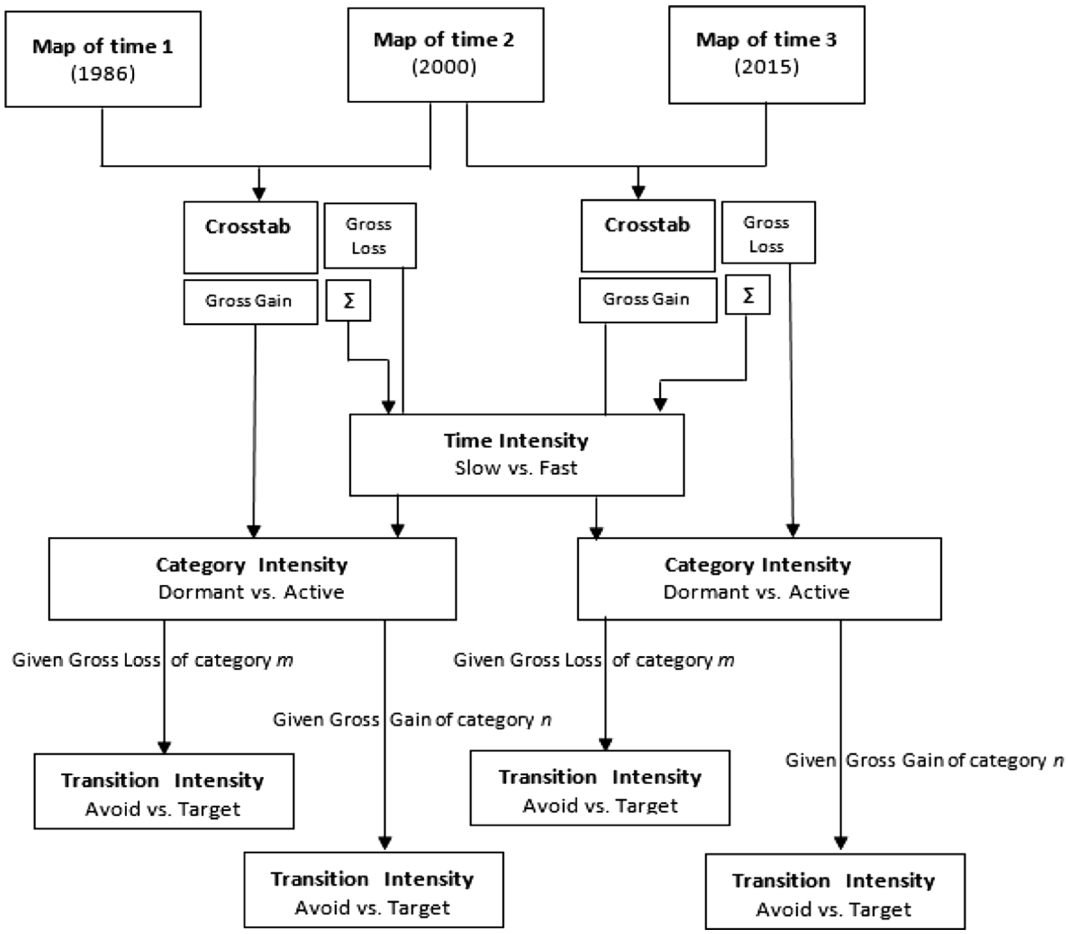

Fig. 1 Methodological flow among the three levels of intensity analysis (from Aldwaik and Pontius Jr 2012)

Table 1 Pixel counts, with underlined numbers on the main diagonal (persistence) and numbers off the main diagonal (Land change) during two-time intervals: 1986–2000 (in italics) and 2000–2015 (in bold)

		Final year of time interval						Initial total	Gross loss
		Cultivation	Grass land	Bare land	Forest	Settlement	Water		
Initial year of time interval	**Cultivation**	*64,753*	*15,909*	*11,315*	*10,735*	*7883*	*710*	*111,305*	*46,552*
		94,433	**14,959**	**15,964**	**4317**	**9206**	**49**	**138,928**	**44,495**
	Grassland	*38,431*	*26,507*	*3564*	*3617*	*2248*	*311*	*74,678*	*48,171*
		36,244	**8519**	**2545**	**1995**	**3856**	**17**	**53,176**	**44,657**
	Bare land	*19,941*	*4605*	*28,428*	*12,282*	*6160*	*320*	*71,736*	*43,308*
		25,450	**2105**	**16,726**	**691**	**2783**	**25**	**47,780**	**31,054**
	Forest	*8463*	*3362*	*2567*	*16,314*	*1857*	*119*	*32,682*	*16,368*
		9495	**2231**	**6302**	**23,283**	**3158**	**7**	**44,476**	**21,193**
	Settlement	*7320*	*2787*	*1901*	*1519*	*2080*	*161*	*15,768*	*13,688*
		8991	**2428**	**3257**	**980**	**4570**	**103**	**20,319**	**15,759**
	Water	*20*	*6*	*5*	*9*	*101*	*4551*	*4692*	*141*
		150	**40**	**225**	**9**	**308**	**5440**	**6172**	**732**
Final total		*138,928*	*53,176*	*47,780*	*44,476*	*20,329*	*6172*	*310,861*	
		174,763	**30,282**	**45,019**	**31,275**	**23,881**	**5641**	**310,861**	
Gross gain		*74,175*	*26,669*	*19,352*	*28,162*	*18,249*	*1621*		*168,228*
		80,330	**21,763**	**28,293**	**7992**	**19,311**	**201**		**157,890**

intensity to a uniform intensity that would exist if the transitions were uniformly distributed among the categories that were available for the transitions. The stationarity of the changes over the intervals across categories and among transitions was examined at each level.

ILI analysis addresses the relative speed of the overall annual rate of change, which is indicated as slow vs. fast (Aldwaik and Pontius 2012; 2013 in press). Equation 1 provides the percentage of the annual change on the landscape for each time interval. When the overall change during all the intervals was uniformly distributed from the initial to the last time point, the uniform annual rate of change on the landscape could be determined (Aldwaik and Pontius 2012) through Eq. 2. If land change was investigated in terms of the total change alone, then this approach would fail to justify the effects of different time intervals on the given land change (Huang et al. 2012), which also indicates the need to consider the intensity of the rate of annual change (Paegelow et al. 2013). The duration of the FTI was 14 years, and the duration of the STI was 15 years. Although the effect of a one-year difference on the land change of the study catchments seemed to be insignificant, this effect was included to better understand when the change was assessed based on the intensity of the rate of annual change.

The size and intensity of each category's gains (Eq. 3) and losses (Eq. 4) during each time interval at the CLI were examined with the respective equations. Accordingly, the intensity of a category's annual gain could be calculated using Eq. 3, and the intensity of the category's annual loss could be calculated from Eq. 4. Equation 5 helps compute the observed intensity of the annual transition from category i to category n during the interval $[Y_t, Y_t + 1]$, which describes the size of category i at time t. Equation 6 provides the hypothesized intensity of the annual transition from all non-n categories to category n during the interval $[Y_t, Y_t + 1]$ relative to the size of all non-n categories at time t. If R_{tin} is greater than W_{tn}, then the gain in n displaces i; if R_{tin} is less than W_{tn}, then the gain in n does not affect i (Aldwaik and Pontius 2012).

According to Aldwaik and Pontius (2012, 2013), transitions from m (Eq. 7) calculate the observed intensity of the annual transition from category m to category j during the interval $[Y_t, Y_t + 1]$ relative to the size of category j at time $t + 1$. Equation 8 computes the hypothesized intensity of the annual transition from category m to all non-m categories during the interval $[Y_t, Y_t$

+ 1] relative to the size of all non-*m* categories at time $t+1$. If Q_{tmj} is greater than V_{tm}, then *j* targets the loss in *m*; if Q_{tmj} is less than V_{tm}, then *j* avoids the loss in *m*. The error at time $t+1$ can explain the deviation between each observed transition intensity and the hypothesized transition intensity (Pontius et al. 2008).

$$S_t = \frac{\text{area of change during interval } [Y_t, Y_t+1]/\text{area of study region}}{\text{duration of interval } [Y_t, Y_t+1]} \times 100\% = \frac{\left\{\sum_{j=1}^{J}\left[\left(\sum_{i=1}^{J} C_{tij}\right) - C_{tjj}\right]\right\} / \left[\sum_{j=1}^{J}\left(\sum_{i=1}^{J} C_{tij}\right)\right]}{Y_{t+1} - Y_t} \times 100\% \quad (1)$$

$$S_t = \frac{\text{area of change during all intervals/area of study region}}{\text{duration of intervals}} \times 100\% = \frac{\sum_{t=1}^{T=1}\left\{\sum_{j=1}^{J}\left[\left(\sum_{i=1}^{J} C_{tij}\right) - C_{tjj}\right]\right\} / \left[\sum_{j=1}^{J}\left(\sum_{i=1}^{J} C_{tij}\right)\right]}{Y_T - T_1} \times 100\% \quad (2)$$

$$G_{tj} = \frac{\text{size of annual gain during}\left[Y_t, Y_{t+1}\right]}{\text{size of } j \text{ at } t+1} \times 100\% = \frac{\left[\left(\sum_{i=1}^{J} C_{tij}\right) - C_{tjj}\right] / (Y_{t+1} - Y_t)}{\sum_{i=1}^{J} C_{tij}} \times 100\% \quad (3)$$

$$L_{ti} = \frac{\text{size of annual loss of i during}\left[Y_t, Y_{t+1}\right]}{\text{size of } i \text{ at } t} \times 100\% = \frac{\left[\left(\sum_{j=1}^{J} C_{tij}\right) - C_{tii}\right] / (Y_{t+1} - Y_t)}{\sum_{j=1}^{J} C_{tij}} \times 100\% \quad (4)$$

$$R_{tin} = \frac{\text{Size of annual transition from } i \text{ to } n \text{ during}\left[Y_t, Y_{t+1}\right]}{\text{size of } i \text{ at } t} \times 100\% = \frac{C_{tin}/(Y_{t+1} - Y_t)}{\sum_{j=1}^{J} C_{tij}} \times 100\% \quad (5)$$

$$W_{tn} = \frac{\text{size of annual gain of } n \text{ during}\left[Y_t, Y_{t+1}\right]}{\text{size } of \text{ not } n \text{ at } t} \times 100\% = \frac{\left[\left(\sum_{i=1}^{J} C_{tin}\right) - C_{tnn}\right] / (Y_{t+1} - Y_t)}{\sum_{j=1}^{J}\left[\left(\sum_{i=1}^{J} C_{tij}\right) - C_{tnj}\right]} \times 100\% \quad (6)$$

$$Q_{tmj} = \frac{\text{size of annual transition from } m \text{ to } j \text{ during}\left[Y_t, Y_{t+1}\right]}{\text{size of } j \text{ at } t+1} \times 100\% = \frac{C_{tmj}/(Y_{t+1} - Y_t)}{\sum_{i+1}^{J} C_{tij}} \times 100\% \quad (7)$$

$$V_{tm} = \frac{\text{size of annual loss of } m \text{ during}\left[Y_t, Y_{t+1}\right]}{\text{size of not } m \text{ at } t+1} \times 100\% = \frac{\left[\left(\sum_{j+1}^{J} C_{tmj}\right) - C_{tmm}\right] / (Y_{t+1} - Y_t)}{\sum_{j+1}^{J}\left[\left(\sum_{j+1}^{J} C_{tij}\right) - C_{tim}\right]} \times 100\% \quad (8)$$

Mathematical symbol notation

The variables of the mathematical symbols in the method are based on the variables in Aldwaik and Pontius Jr (2013).

T	Number of time points
Y	Year at time point *t*
t	First time point index in the interval [*Yt*,*Yt* + 1], and *t* ranging from *1* to *T*-1
J	Number of land-change categories
i	Category index at an interval's first/initial time point
j	Category index at an interval's last/final time point
m	Losing category index for the selected transition
n	Gaining category index for the selected transition
Ctij	Number of elements that transition from category *i* to category *j* during interval [*Yt*,*Yt* + 1]
St	Annual change during interval [*Yt*,*Yt* + 1]
U	Annual uniform change during extent [*Y1*,*YT*]
Gtj	Annual gain intensity of category *j* during interval [*Yt*,*Yt* + 1] relative to the size of category *j* at time *t* + 1
Lti	Annual loss intensity of category *i* during interval [*Yt*,*Yt* + 1] relative to the size of category *i* at time *t*
Rtin	Annual transition intensity from category *i* to category *n* during interval [*Yt*,*Yt* + 1] relative to the size of category *i* at time *t*
Wtn	Uniform intensity of annual transition from all non-*n* categories to category *n* during interval [*Yt*,*Yt* + 1] relative to the size of all non-*n* categories at time *t*
Qtmj	Intensity of annual transition from category *m* to category *j* during interval [*Yt*,*Yt* + 1] relative to the size of category *j* at time *t* + 1
Vtm	Uniform intensity of annual transition from category *m* to all non-*m* categories during interval [*Yt*,*Yt* + 1] relative to the size of all non-*m* categories at time *t* + 1

Results and discussion

All the land categories experienced gains and losses in different proportions across the two time intervals (Fig. 2). When land change was assessed at the general landscape level, cultivation was the leading land-gaining category (Table 1). Grassland, followed by bare land were the main losing categories. The gains in cultivated land were 6675.7 and 7229.7 ha during the FTI and STI, respectively. These categories also lost approximately 4189.7 and 4004.5 ha of land during the FTI and STI, respectively, to other land categories. Thus, the same land-cover category experienced a net gain of 2486 ha during the FTI and 3225 ha during the STI (Table 1). Forest category gains of 2534.6 ha and losses of 1473 ha occurred during the FTI. For the same land category, gains of 719.3 ha and losses of 1907.4 ha occurred during the STI. Therefore, the forest category experienced a net gain of 1061.5 ha during the FTI and a net loss of 1188 ha during the STI. Grassland had 2400 ha of gains and 4335.4 ha of losses during the FTI, and 1958.7 ha of gains and 4019.2 ha of losses occurring during the STI.

Consequently, this category exhibited a net loss of 1935.2 ha during the FTI and 2060.5 ha during the STI throughout the study period. At the same time, bare land exhibited 2546.8 ha of gains and 2794.9 ha of losses during the STI in addition to 1741.7 ha of gains and 3897.7.2 ha of losses during the FTI, indicating a net loss of 2156 ha during the FTI and 248.5 ha during the STI. The settlement category had net gains of 410.5 and 319.9 ha during the FTI and STI, respectively.

The water category exhibited a net gain of 133.2 ha during the FTI and a net loss of 47.79 ha during the STI. These changes seem subtle but are significantly large (net gain of 31.55% and net loss of 8.6%) compared to the category's initial total area during each interval (i.e., 422.28 ha in the FTI and 555.48 ha in the STI). The net gain in the water category during the FTI was attributed to the construction (1998) and commissioning (1999) of new sediment trapping by the Dire dam in the upper portion of the Legedadie catchment. However, the net loss afterward might have reflected a reduction in the reservoir water volume depending on the magnitude of evaporation and total sediment accumulation. Reservoirs' sedimentation process brings two major changes that causes reduction in water yield: storage capacity loss and morphological changes. The storage capacity reduction increased spillway overflow losses (Michalec 2015; DE ARAÚJO et al. 2006), and the morphological changes by sedimentation reshapes reservoirs and makes more shallow and open which induces the water

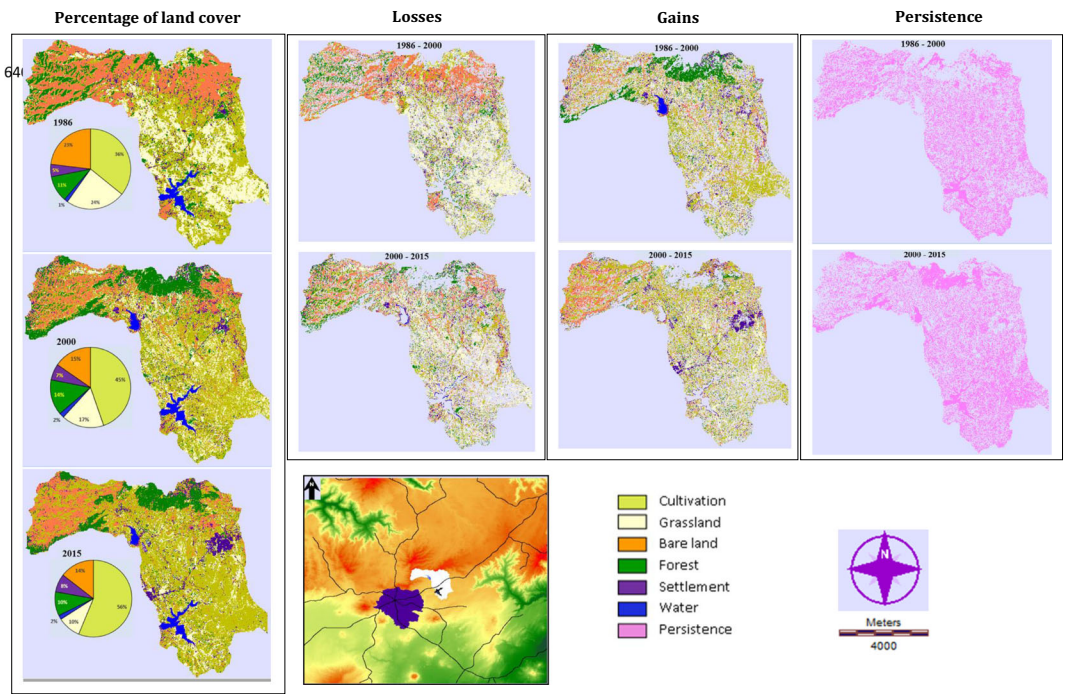

Fig. 2 Percentage of land categories at three time points and changes during two

to warmth quickly and increases evaporation loss (DE ARAÚJO et al. 2006). A reduction in storage capacity normally implies a reduction in water availability given reservoirs less space to store runoff water during the rainy season, leading to greater spillway overflows (Michalec 2015; DE ARAÚJO et al. 2006). The spill overflow was 42.4 and 23.5 Mm^3 per year for the Legedadie and Dire reservoirs, respectively (MPR 2011), which can be considered as a loss for the reservoir in terms of water availability. The very steep slopes in the upper portions of the catchments and poor environmental-conservation status of the area both augment soil erosion (Elala 2011). Furthermore, the moderate residence time of reservoirs (nearly 1 year for new additions of water from rainfall runoff) is sufficient for sediments to effectively settle, enhancing their trap efficiency.

ILI analysis

Figure 3 shows the results of the ILI analysis. Significant land change occurred across the entire study period (Fig. 3). The results revealed that the extent of the total land change was slightly larger during the FTI than that during the STI, even though the FTI was shorter than the STI by 1 year. The total land change percentage of the domain was approximately 54% for the initial (1986–2000) and 51% for the latter (2000–2015) time intervals.

If land changes across the catchments were uniformly distributed during all the intervals, then the annual rate of land change would equal 3.63%, as shown by the uniform line in Fig. 3. Nevertheless, the rate of change in the study catchments was not uniform, as shown in Fig. 3. The right sides of the bars displayed an annual rate of change that was faster (i.e., 3.87% of the interval's domain) during the FTI than that during the STI (i.e., 3.40% of interval's domain). The STI was 1 year longer than the FTI, but the land change was relatively fast and intensive during the FTI than that during the STI. Thus, the land change process in the catchments was mainly governed by the intensity of change at some point during the period rather than the entire time duration of the intervals. For example, faster land change during the FTI was not mainly caused by its time duration but rather by the high intensity of change during this interval.

The bars for the two intervals did not equal the uniform line at 3.63%, so the rate of annual change was not uniformly distributed and thus not perfectly stationary in the ILI analysis. CLI analysis can further identify the categories that most contribute to the intensity of change at the interval level (or whether the high intensity of change at the interval level would encompass all the categories or be limited to certain categories alone).

CLI analysis

In the graph below (Fig. 4), cultivation exhibited a noticeable gain during both intervals, whereas obvious losses were observed in grassland and bare land during both intervals and in forest during the STI. Grassland was the category with the largest losses in the two time intervals, followed by bare land.

The bar graph on the left side shows only the observed gains and losses but does not show the intensities of these changes. A deeper understanding of systematic land transitions requires considering the change intensity (i.e., gain intensity vs. loss intensity), which enables one to compare the size of a change with the intensity of change. Therefore, each category's gain was divided by the size of the category at the subsequent time for the

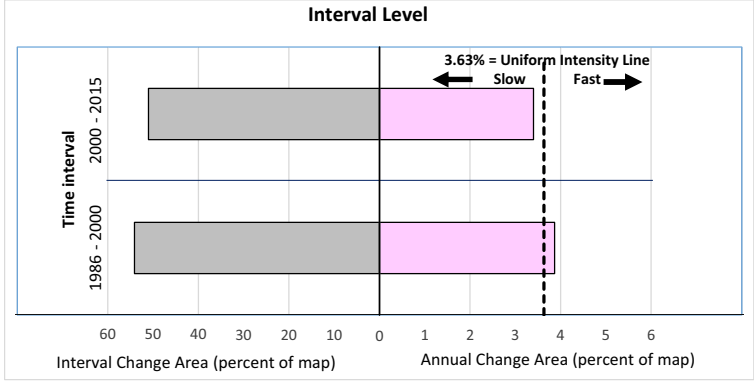

Fig. 3 Interval change area and annual change area of the two-time intervals: 1986–2000 and 2000–2015

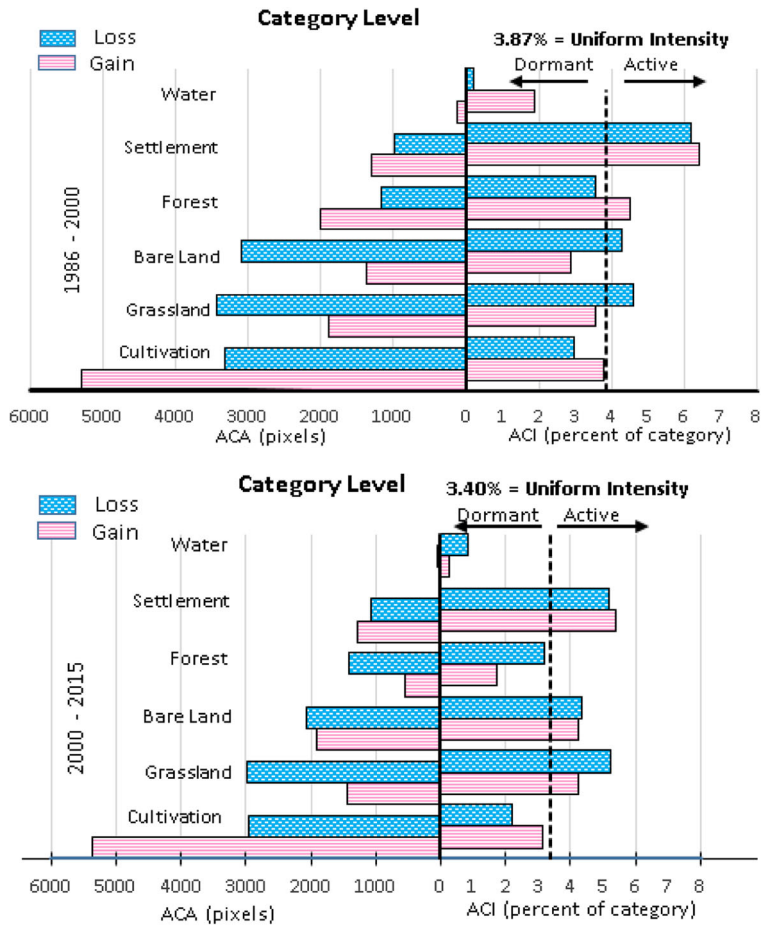

Fig. 4 Annual change area and annual change intensity between 1986 and 2000 (upper) and between 2000 and 2015 (lower)

gain intensity. However, each category's loss was divided by the size of the category at the initial time for the loss intensity. The right side of the figure provides detailed information regarding the change intensity of a category's gains and losses. According to the net effect of the gross gains and losses, cultivation, forest, settlement, and water were the gain categories during the FTI, while cultivation and settlement were the only gain categories during the STI.

In both time intervals, cultivation was the largest gain category. The gross gains in cultivation were 23.9% (6675.75 ha FTI^{-1}) and 25.8% (7229.7 ha STI^{-1}) of the domain. Hence, this category, which exhibited the largest gross gains among the land-cover types during the FTI, maintained continuous gains, even more so than other categories during the STI. When disaggregated by the average annual change, this class gained 1.7% (477 ha $year^{-1}FTI^{-1}$) and 1.73% (482 ha $year^{-1}$ STI^{-1}) of the domain without considering the annual average losses.

We must observe the net change as the effect of gains and losses to more deeply understand the change process. Cultivation was generally the net gaining category throughout the study period, exhibiting net gains of 8.89% (2486 ha FTI^{-1}) and 11.5% (3225 ha STI^{-1}) in the domain across the time spans. In other words, the annual average net gain in cultivation was approximately 0.6% (177.7 ha $year^{-1}$ FTI^{-1}) and 0.8% (215 ha $year^{-1}$ STI^{-1}) of the domain. However, the annual gain intensity of cultivation was dormant over both time ranges, as shown in Fig. 4, which indicates that the significantly large comparative gain in this category could be partially attributed to its relatively large area at the initial time. Thus, if each category gained uniformly, cultivation would proportionately gain more relative to the size of its category at the beginning.

Forest had the second largest gained area from the other land categories during the FTI, followed by settlements throughout the entire period and water during the FTI. The gross gain in forest was approximately 9.6%

(2534.6 ha FTI^{-1}), but 6.8% (1907.4 ha STI^{-1}) of the domain was in its gross loss counterpart. On average, the forest category possessed 0.6% (181 ha $year^{-1}FTI^{-1}$) and lost 0.5% (127 ha $year^{-1}STI^{-1}$) over the entire landscape annually. When assessed by the net change percent, the same land category had a net gain of 3.8% (1061.5 ha FTI^{-1}) and a net loss of 4.25% (1188 ha STI^{-1}) in the domain. In other words, forests exhibited 0.3% net gain (76 ha $year^{-1}$ FTI^{-1}) and net loss (79 ha $year^{-1}$ STI^{-1}) annually. Consistent with this result, the annual gain intensity in the forest category was active during the FTI but dormant during the STI. Thus, the gains and losses in forest during the FTI and STI were not caused by the relative size and proportionate net change in the forest category but rather with the strong efforts of reforestation and conversion of degraded areas by *Eucalyptus* trees during the initial period of the FTI. This result is consistent with the massive scale of afforestation and soil conservation on farms and public lands that occurred in the country during the Derg regime and the subsequent countrywide deforestation soon after the fall of the regime (Eshetu 2013).

Additionally, settlement grossly gained 5.9% (1642 ha FTI^{-1}) and 6.2% (1738 ha STI^{-1}), whereas water gained 0.5% gross (146 ha FTI^{-1}) in the domain. Therefore, the annual gains in these categories as a percentage of the domain were 0.4% for settlement in both intervals (117 ha $year^{-1}$ FTI^{-1} and 116 ha $year^{-1}$ STI^{-1}) and 0.04% for water during the FTI.

When disaggregating by net change, settlement had a net gain of 1.5% (410.5 ha FTI^{-1}) and 1.1% (319.7 ha STI^{-1}) of the domain. In other words, the same land category annually experienced a net gain of 0.1% during each time interval (i.e., 29 ha $year^{-1}$ FTI^{-1} and 21 ha $year^{-1}$ STI^{-1}) in the domain. Similarly, water had a net gain of 0.5% (133.2 ha FTI^{-1}) of the domain during the FTI. Settlement was the most active category during both time intervals in terms of annual gain intensity, which implies that this category was gaining actively and more intensively despite its relatively small size at the initial time. Water gained with greater intensity during the FTI than during the STI. However, the gain in water was entirely dormant during both time intervals. The gain in water during the FTI was, therefore, a reflection of the newly built-up and the commissioning of the Dire reservoir in 1998, which represents a one-time possession that led to the dormancy of the category.

Considering the net effects of the changes, the grassland, bare land, and forest categories were among the major loss categories on the landscape. Grassland and bare land remained the principal loss categories during both the FTI and STI, whereas forest was lost during the STI. Within the total domain, grassland grossly lost 15.5% (4335.6 ha FTI^{-1}) and 14.4% (4019 ha STI^{-1}) and bare land lost 13.9% (3897.8 ha FTI^{-1}) and 10% (2794.9 ha STI^{-1}). When interpreting the results annually, grassland lost 1.1% (310 ha $year^{-1}$ FTI^{-1}) and 1% (268 ha $year^{-1}$ STI^{-1}) on average. Similarly, the average annual losses in the bare land category as a percentage of the domain were estimated at 1% (278 ha $year^{-1}$ FTI^{-1}) and 0.7% (186 ha $year^{-1}$ STI^{-1}). These losses were larger during the FTI than during the STI. These categories experienced both losses and gains, so we must investigate the net effects of these losses to better understand the change process. When assessed based on the net change, grassland had a net loss of 6.9% (1935 ha FTI^{-1}) and 7.4% (2060.5 ha STI^{-1}), whereas bare land had a net loss of 7.7% (2156 ha FTI^{-1}) and 0.9% (2,48.5 ha STI^{-1}) within the total domain. Alternatively, grassland had a net annual loss of 0.5% during each interval (138 ha $year^{-1}$ FTI^{-1} and 137 ha $year^{-1}$ STI^{-1}), whereas bare land lost 0.6% (154 ha $year^{-1}$ FTI^{-1}) and 0.1% (16 ha $year^{-1}$ STI^{-1}) within the total domain. The annual loss intensities of the grassland and bare land categories were active during all the time intervals, indicating that the changes were not caused by their proportionate size at the initial time but rather by being intensively targeted by other categories.

Forests exhibited losses only during the STI. The gross loss for this category was approximately 6.8% (1907.4 ha STI^{-1}), which indicates an estimated average annual loss in this category of 0.5% (127 ha $year^{-1}$ STI^{-1}) when not considering the net effect of changes. When considering the net effects of changes (including gains), forests lost a net of 4.3% (1188 ha STI^{-1}) within the domain, which implies that the average annual net loss of forest during the same time interval was approximately 0.3% (79 ha $year^{-1}$ STI^{-1}). Nevertheless, the loss intensity of forest during the STI was dormant, which signifies that forest loss may have occurred during a specific short time step within this interval instead of throughout this interval.

Categories with the largest annual gain may not have the most active annual intensity of gains. At the same time, categories with the greatest annual losses may not have the most dormant annual intensity losses. For example, the bar for the gain of cultivation to the left extended far beyond the other bars, indicating the largest

annual gain in the category within both time intervals; however, its bar for the annual gain intensity extended short of the uniform line, signifying that it was dormant across all the time intervals. The large gain in this category, therefore, was attributed to its large area at the initial time. Hence, when all the categories gained uniformly with the same intensity, this category might have also experienced the largest gains relative to its initial size. Similarly, the bar for the annual gains in settlement to the left was shorter than the other bars, indicating smaller gains than in other categories within these intervals. However, the bar to the right for the annual gain intensity extended beyond the uniform line, implying that its gain intensity was very active during both intervals and indicating that this intensity analysis provided insight to explain the relative sizes for the losses and gains. Therefore, we should investigate the intensity side of the bar graph to assess whether the massive annual change was simply caused by the large size of the categories or the intensiveness of changes within the categories.

The isolated examination of losses or gains without considering the net effects of changes may cause a given category to appear to be the largest gainer or loser. For example, in Fig. 4, settlement appeared to lose while bare land seemed to gain during the STI. However, when assessed with the net effects of changes, the former category was the absolute gainer, whereas the latter category experienced purely losses.

Stationarity at the category level

At the CLI analysis, none of the land categories exhibited perfect stationarity because each category's change during the intervals did not equal the annual uniform change during the intervals. In other terms, a category's annual intensity bar did not end up at the uniform intensity line. However, stationarity existed in some categories losses or gains depending on the extent of their annual change intensity though imperfectly. Accordingly, both the gains and losses in the water and cultivation categories remained dormant during both intervals. Similarly, the gains and losses in settlement were active during all the intervals. Therefore, these categories were stationary in terms of the annual intensity of both gains and losses, but they were not perfect. Additionally, the annual intensity of losses in forest were dormant, whereas those for bare land and grassland were active during both intervals. Thus, forest, bare land, and grassland were stationary in terms of the annual intensity of losses. In terms of the annual intensity of gains, forest was active during the FTI but dormant during the STI. Similarly, bare land and grassland were dormant during the FTI and active during the STI. Therefore, these categories were not stationary in terms of their annual gain intensities.

TLI analysis

Land change in terms of gains and losses across the catchments predominantly appeared between cultivated land (gains) and grassland (losses). Thus, TLI analysis was utilized to focus on the transition from other categories to cultivation and the transition from grassland to all other categories. In short, transition ***to*** cultivation was assessed first, followed by transition *from* grassland.

Transition "to" cultivation

Figure 5 shows the rate and transition intensity of categories that cultivation displaced annually. According to the size of the area that cultivation gained annually, gains were observed from grassland and then from bare land, followed by settlement and forest (left side of Fig. 5).

Similarly, the annual transition intensity indicated the strength of the transitions and revealed that cultivation targeted grassland during both time intervals and, to some extent, bare land (STI) and settlement (FTI). Hence, substantial gains in cultivation from grassland during both time intervals and from bare land during the STI were not caused by these categories' relatively large area at the initial time but rather by the gains in cultivation causing these categories to intensively lose area (right side of Fig. 5). The large area transition from bare land to cultivation during the FTI, which is represented by the annual transition on the graph, was not practically reflected by the annual transition intensity on the same graph. Thus, unlike the STI, the large area losses from bare land to cultivation during the FTI were attributed to its relatively large area at the initial time. Thus, if all the categories lost uniformly, then bare land would lose more annually relative to its size.

The annual transition intensity of the graph also indicated that settlement was displaced by cultivation during the FTI but not during the STI. However, the bar graph of the annual transition area of settlement appeared short, indicating that even though this category

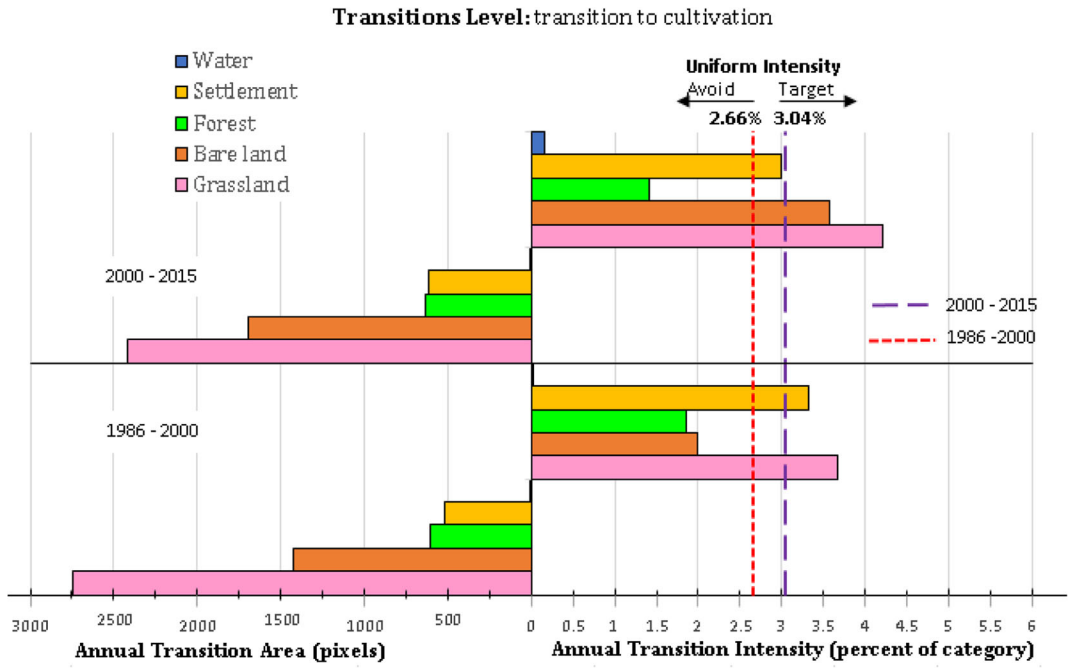

Fig. 5 Annual transition area and annual transition intensity to cultivation in the two time intervals: 1986–2000 and 2000–2015

was targeted, its contribution was small relative to its initially small total area. The loss in this category to cultivation during the FTI was difficult to discern. Nevertheless, we expect that this result might have been associated with the resettlement program during the construction of the Dire dam water-supply project, which was involved in the expropriation of settlement land for the construction of the dam and a closure site for a sanitary zone during the FTI. Although full data could not be obtained, the resettlement program for the construction of the Dire dam water-supply projects displaced many households (Bayrau and Bekele 2007). The resettled residents were provided, among other compensations, 6 Eth. birr per sq. m, 250 sq. m of land per household and 2000 Eth. Birr per household for disturbances (Bayrau and Bekele 2007). Later, the closure fences have damaged because of a lack of proper monitoring which let the locals to use part of the sanitary zone for cultivation, as observed during the field campaign used part of the sanitary zone for cultivation.

Stationarity during the transition to cultivation At the level of transition to cultivation, no categories were perfectly stationary over time because none of the annual transition intensities equaled the annual uniform intensity. However, the gains in cultivation from grassland were stationary over time in the intensity analysis' definition of the term. This result occurred because the gain in cultivation targeted grassland during all the intervals. However, bare land was avoided during the FTI and targeted during the STI. Settlement was targeted during the FTI and avoided during the STI for appropriation by cultivation. Therefore, the transition to cultivation from bare land and settlement was not stationary over time. Similarly, forest and water (impossible to cultivate) were entirely avoided by cultivation for appropriation during the entire period; therefore, the transition to cultivation from these categories was stationary.

Transitions "*from*" grassland

Figure 6 displays the results for the transitions from grassland during both intervals, including the gains from grassland for each of the gain categories. In terms of the size of the annual transition, when grassland shrunk, the largest transition was to cultivation, followed by smaller transitions to bare land, settlement and forest. Similarly, in terms of the annual transition intensities, the bars for cultivation extended far to the right of the uniform line during both the FTI and STI. However, the transition-intensity bars for the remaining categories remained short of the uniform line during both the FTI and STI. Any grassland losses occurred tended to be mostly to cultivation compared to any other categories across the

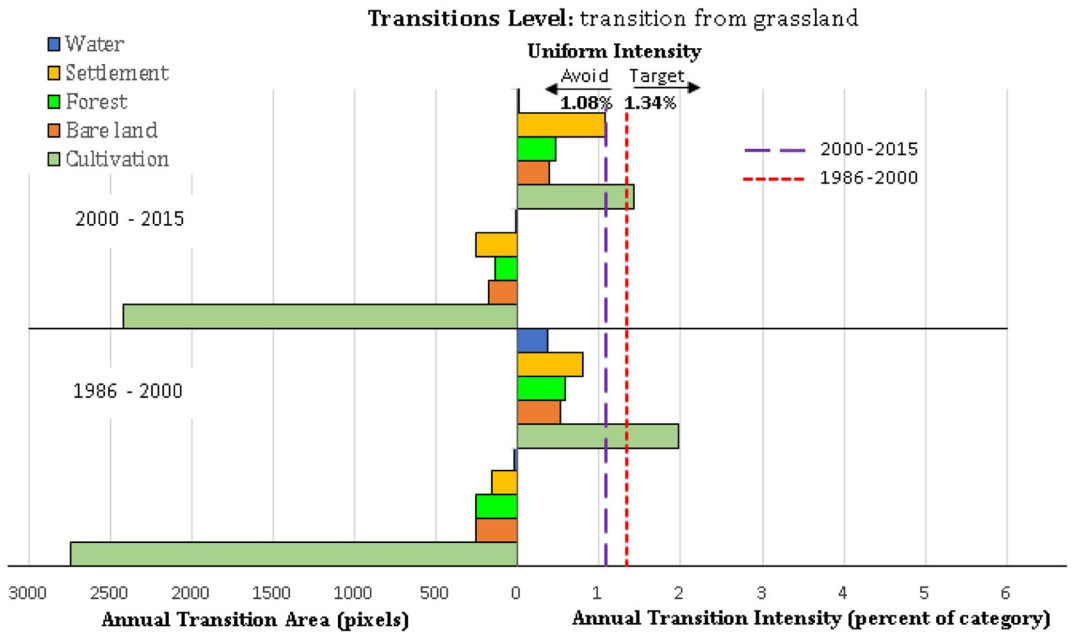

Fig. 6 Annual transition area and annual transition intensity from grassland during the two time intervals: 1986–2000 and 2000–2015

entire time interval. Thus, the intensive loss of grassland targeted cultivation and avoided other categories over all the time intervals. Hence, substantial gains in cultivation from grassland did not occur because of this category's relatively large percentage on the landscape at the initial time but mainly because of grassland being intensively displaced by cultivation while avoiding other categories.

Stationarity during transitions from grassland When grassland intensively decreased, any transitions involved were targeting the cultivation category during both the FTI and STI, and avoided all other categories across the two intervals. Therefore, all the transitions from grassland to other categories indicated stationarity across the two time intervals. However, none of these transitions were perfectly stationary.

Implications

Land change is necessary and essential for economic development and social progress (Wu 2008). Land change is perhaps the most pervasive socioeconomic force that drives changes and provides many economic and social benefits but often comes with substantial costs to the environment and the degradation of ecosystems. Deforestation, the expansion of built-up areas, settlements, cultivation, and other human activities can substantially alter the landscape. Such disturbances of the land affect important ecosystem processes and services that end up with wide-ranging and long-term consequences. For example, cultivation practices have potentially severe ecosystem consequences and can cause water pollution. Runoff from agricultural lands is a leading source of water pollution (Lubowski et al. 2006). Thus, the conversion of grasslands and forests to cultivation exacerbates such consequences.

Urbanization obviously negatively affects water quality because of increased sewage water and industrial wastewater (Wagner et al. 2013). Urban runoff often transports toxic contaminants, sediment, and nutrients and can cause both water pollution and large variations in stream flow and water temperatures (Lubowski et al. 2006). Thus, the conversion of farmland and forests to urban development further intensifies these problems. Deforestation and the loss of grass cover affect the hydrological cycle and increase soil erosion, runoff, and flooding, which lead to siltation and water pollution.

The Legedadie and Dire reservoirs, which are the major sources of potable water to the nation's capital city, Addis Ababa, are currently experiencing severe pollution. The high pollution and sedimentation in these reservoirs leads to water-supply shortages in the city. Thus, land-change processes in the catchment facilitate the physical removal of soil (Gebresamuel et al. 2010) and accelerate the deterioration of the reservoirs' water quality and quantity (Kebede 2012). According to the

World Bank information document,[2] the water-treatment costs of the municipality have increased four-fold over the past decade. Today, the potable water demand of the city is growing nearly three times faster than the water-supply rate (MPR 2011), which is a warning sign that sound planning and the management of existing and additional water-supply sources are required. The land-change phenomena that have been recently observed in the catchment have significant implications for the water-supply systems in Addis Ababa. Further studies should address the drivers of perceived land changes from the perspective of underlying and related factors.

Conclusions

The rate of overall land change was fast during the FTI but slower during the STI. Cultivation and settlements were the major net-gain categories throughout the study period. Nevertheless, the annual gain intensity was active for settlements and dormant for cultivation. However, grassland and bare land were the dominant net-loss categories during the entire study period. The annual loss intensities in these categories were always active throughout the FTI and STI. None of the land categories showed perfect stationarity in all three levels of analysis across the study period. However, stationarity did exist (but not perfectly) in some categories among the three levels of analysis. Moreover, the categories encountered a one-step direct transition. Direct transitions were involved from grassland to cultivation, from bare land to cultivation, and from settlement to cultivation. All the direct transitions from grassland to cultivation were involved during both the FTI and the STI, which implies that grassland was the most displaced category by cultivation during both time intervals. The transition from bare land to cultivation initiated during the STI, signifying that the increasing population and pressure on land resources led to a scarcity of cultivated land and, thus, encroachment onto infertile bare surfaces.

This study supports the sound planning and management of existing and additional water-supply sources. Further studies that identify the drivers of land change are imperative. Generally, intensity analysis helps identify and measure the rate of land changes across time intervals, identify dormant and active categories of land change, and detect the most targeted and avoided categories at the three levels of measurement.

[2] Project Information Document (PID) Appraisal Stage, Urban Water Supply and Sanitation Project Report No.: AB2840. Washington, D.C.: World Bank Group.

Acknowledgements We acknowledge the Borlaug Leadership Enhancement in Agricultural Program (Borlaug LEAP) for providing a fellowship to realize this research project. The International Foundation for Science (IFS) also funded this research project under Grant No. W/5386-2, and their core financial support is highly appreciated. Moreover, we express our appreciation to Arba Minch University, Ethiopia, for offering a sponsorship and the Ethiopian Institute of Architecture, Building Construction, and City Development, Addis Ababa University, Ethiopia, for its key role in grant administration.

References

Achard, F., Eva, H., Stibig, H. J., Mayaux, P., Gallego, J., Richards, T., et al. (2002). Determination of deforestation rates of the world's humid tropical forests. *Science, 297*, 999–1002.

Aldwaik, S. Z., & Pontius Jr., R. G. (2012). Intensity analysis to unify measurements of size and stationarity of land changes by interval, category, and transition. *Landscape and Urban Planning, 106*, 103–114.

Aldwaik, S. Z., & Pontius Jr, R. G. (2013). Map errors that could account for deviations from a uniform intensity of land change. *International Journal of Geographical Information Science., 27*(9), 1717–1739.

Alemayehu, S.T., Dorosh, P. and Sinafikeh, A., 2011. Crop production in ethiopia: regional patterns and trends. development strategy and governance division, international food policy research institute, Ethiopia Strategy Support Program II (No. 0016). ESSP II Working Paper.

Andualem, G., & Yonas, M. (2008). Prediction of sediment inflow to Legedadi Reservoir using SWAT watershed and CCHE1D sediment transport models. *Nile Basin Water Engineering Scientific Magazine, 1*, 2008.

Bayrau, A. and Bekele, G., 2007. Households' willingness to resettle and preference to forms of compensation for improving slum areas in Addis Ababa City. Development, 2000.

Boyd, D. S., & Danson, F. M. (2005). Satellite remote sensing of forest resources: Three decades of research development. *Progress in Physical Geography, 29*(1), 1–26.

Boyle, S. A., Kennedy, C. M., Torres, J., Colman, K., Perez-Estigarribia, P. E., & Noé, U. (2014). High-resolution satellite imagery is an important yet underutilized resource in conservation biology. *PLoS One, 9*(1), e86908.

Carleer, A. P., Debeir, O., & Wolff, E. (2005). Assessment of very high spatial resolution satellite image segmentations. *Photogrammetric Engineering & Remote Sensing, 71*(11), 1285–1294.

Dadi, D., Stellmacher, T., Azadi, H., Abebe, K. and Senbeta, F., 2015. e Impact of Industrialization on Land Use and

Livelihoods in Ethiopia: Agricultural Land Conversion around Gelan and Dukem Town, Oromia Region.

Dadi, D., Azadi, H., Senbeta, F., Abebe, K., Taheri, F., & Stellmacher, T. (2016). Urban sprawl and its impacts on land use change in Central Ethiopia. *Urban Forestry & Urban Greening, 16*, 132–141.

DE ARAÚJO, J. C., GÜNTNER, A., & Bronstert, A. (2006). Loss of reservoir volume by sediment deposition and its impact on water availability in semiarid Brazil. *Hydrological Sciences Journal, 51*(1), 157–170.

Durieux, L., Lagabrielle, E., & Nelson, A. (2008). A method for monitoring building construction in urban sprawl areas using object-based analysis of Spot 5 images and existing GIS data. *ISPRS Journal of Photogrammetry and Remote Sensing, 63*(4), 399–408.

Eastman, J.R. (2016). IDRISI Terrset Manual. Clark Labs-Clark University: Worcester, MA, USA.

Eggenberger, W. and Hunde, M., 2001. 2001 Belg Season in North-Central Ethiopia: Rains late but farmers remain optimistic. Report of a joint UN-EUE/MoA/FAO mission undertaken from 19—29 March 2001.

Elala, D., 2011. Vulnerability assessment of surface water supply systems due to climate change and other impacts in Addis Ababa, Ethiopia.

Eshetu, A. A. (2013). Forest resource management systems in Ethiopia: historical perspective. *International Journal of Biodiversity and Conservation, 6.2*(2014), 121–131.

Frantz, D., Röder, A., Stellmes, M. and Hill, J. (2016). An operational radiometric landsat preprocessing framework for large-area time series applications. IEEE Transactions on Geoscience and Remote Sensing, 54(7), pp.3928–3943.

Gebresamuel, G., Singh, B. R., & Dick, O. (2010). Land-use changes and their impacts on soil degradation and surface runoff of two catchments of northern Ethiopia. *Plant Soil Science, 60*(3), 211–226.

Gergel, S. E., & Turner, M. G. (2000). *Learning landscape ecology: a practical guide to concepts and techniques*. New York, NY: Springer.

Hansen, M. C., Shimabukuro, Y. E., Potapov, P., & Pittman, K. (2008). Comparing annual MODIS and PRODES forest cover change for advancing monitoring of Brazilian forest cover. *Remote Sensing of Environment, 112*, 3784–3793.

Harsanyi, J.C., Farrand, W. and Chang, C.I. (1994). April. Detection of subpixel spectral signatures in hyperspectral image sequences. In Annual Meeting, Proceedings of American Society of Photogrammetry & Remote Sensing (pp. 236–247).

Huang, J., Pontius, R. G., Li, Q., & Zhang, Y. (2012). Use of intensity analysis to link patterns with processes of land change from 1986 to 2007 in a coastal watershed of Southeast China. *Applied Geography, 34*, 371–384.

Kebede, W. (2012). Watershed management: an option to sustain dam and reservoir function in Ethiopia. *Journal of Environmental Science and Technology, 5*(5), 262–273.

Lambin, E.F. and Geist, H.J. eds., 2008. Land-use and land-cover change: local processes and global impacts. Springer Science & Business Media.

Liu, J., Heiskanen, J., Aynekulu, E., & Pellikka, P. K. E. (2015). Seasonal variation of land cover classification accuracy of Landsat 8 images in Burkina Faso. *The International Archives of Photogrammetry, Remote Sensing and Spatial Information Sciences, 40*(7), 455.

Lu, D., Hetrick, S., & Moran, E. (2010). Land cover classification in a complex urban-rural landscape with QuickBird imagery. *Photogrammetric Engineering & Remote Sensing, 76*(10), 1159–1168.

Lubowski, R.N., Vesterby, M., Bucholtz, S., Baez, A., and Roberts, M.J. 2006. Major uses of land in the United States, 2002. Economic Information Bulletin No. (EIB–14).

Macleod, R. D., & Congalton, R. G. (1998). A quantitative comparison of change detection algorithms for monitoring eelgrass from remotely sensed data. *Photogrammetric Engineering and Remote Sensing, 64*(3), 207–216.

Mahavir, D., 2000. High (spatial) resolution vs. low resolution images: a planner's view point. International archives of photogrammetry and Remote Sensing, 33(7).

Meyer, W. B., & Turner II, B. L. (2002). The earth transformed: trends, trajectories, and patterns. In R. J. Johnston, P. J. Taylor, & M. J. Watts (Eds.), *Geographies of global change: remapping the world* (2nd ed., pp. 364–376). Oxford: Blackwell.

Michalec, B. (2015). Evaluation of an empirical reservoir shape function to define sediment distributions in small reservoirs. *Water, 7*(8), 4409–4426.

MPR (FDRE Master Plan Review). 2011., Catchment Rehabilitation and Awareness Creation for Geffersa, Legedadi, and Dire Catchment Areas, urban water supply and sanitation project report.

Munsi, M., Malaviya, S., Oinam, G., & Joshi, P. K. (2010). A landscape approach for quantifying land-use and land cover change (1976–2006) in middle Himalaya. *Regional Environmental Change, 10*, 145–155.

Paegelow, M., Camacho Olmedo, M. T., Mas, J. F., Houet, T., & Pontius Jr, R. G. (2013). Land change modelling: moving beyond projections. *International Journal of Geographical Information Science, 27*(9), 1691–1695.

Pontius, R. G., Jr., & Malizia, N. 2004. Effect of category aggregation on map comparison. Lecture Notes in Computer Science 3234. In M. J. Egenhofer et al. (Eds.), GIScience 2004 (pp. 251–268).

Pontius, R. G., Boersma, W., Castella, J. C., Clarke, K., de Nijs, T., Dietzel, C., Duan, Z., Fotsing, E., Goldstein, N., Kok, K., & Koomen, E. (2008). Comparing the input, output, and validation maps for several models of land change. *The Annals of Regional Science, 42*(1), 11–37.

Redo, D., Millington, A. C., & Hindery, D. (2011). Deforestation dynamics and policy changes in southeastern Bolivia. *Land Use Policy, 28*, 227–241.

Rogan, J., & Chen, D. (2004). Remote sensing technology for mapping and monitoring land-cover and land-use change. *Progress in Planning, 61*, 301–325.

Romero-Ruiz, M. H., Flantua, S. G. A., Tansey, K., & Berrio, J. C. (2011). Landscape transformations in savannas of northern South America: Land use/cover changes since 1987 in the Llanos Orientales of Colombia. *Applied Geography, 32*, 766–776.

Takada, T., Miyamoto, A., & Hasegawa, S. F. (2010). Derivation of a yearly transition probability matrix for land-use dynamics and its applications. *Landscape Ecology, 25*(4), 561–572.

Tan, K., Li, E., Du, Q. and Du, P. (2014). Hyperspectral image classification using band selection and morphological

profiles. *IEEE Journal of Selected Topics in Applied Earth Observations and Remote Sensing, 7*(1), pp.40–48.

Turner, B.L., 2006. Land change as a forcing function in global environmental change. Our Earth's changing land: an encyclopedia of land-use and land-cover change, 1.

Turner II, B. L. (2002). Toward integrated land-change science: Advances in 1.5 decades of sustained international research on land-use and land cover change. In *W. Steffen, J et. Al., (Eds.), challenges of a changing earth. Proceedings of the global change Open Science conference, Amsterdam, the Netherlands* (pp. 21–26). Berlin: Springer.

Verburg, P. H., Van De Steeg, J., Veldkamp, A., & Willemen, L. (2009). From land cover change to land function dynamics: a major challenge to improve land characterization. *Journal of Environmental Management, 90*(3), 1327–1335.

Wagner, P. D., Kumar, S., & Schneider, K. (2013). An assessment of land use change impacts on the water resources of the Mula and Mutha rivers catchment upstream of Pune, India. *Hydrology and Earth System Sciences, 17*(6), 2233–2246.

WELCH, R. (1982). Spatial resolution requirements for urban studies. *International Journal of Remote Sensing, 3*(2), 139–146.

Wu, J., 2008. Land use changes: economic, social, and environmental impacts.

Wu, K. Y., Ye, X. Y., Qi, Z. F., & Zhang, H. (2013). Impacts of land use/land cover change and socioeconomic development on regional ecosystem services: The case of fast-growing Hangzhou metropolitan area, China. *Cities, 31*, 276–284.

Yang, Y., 2013. Towards robust representation and classification of low-resolution image and video data.